Low Temperature Hydrothermal Fabrication of Tungsten Trioxide on the Surface of Wood with Photochromic and Superhydrophobic Properties

Minglei Sun,[a,b] and Kuiyan Song [a,*]

Tungsten trioxide (WO_3), which is a semiconductor, was hydrothermally synthesized onto the surface of wood. After the *in-situ* synthesis of WO_3 nanoparticles on the wood surface, the wood exhibited photochromic and superhydrophobic properties. The WO_3 nanostructures were fabricated on wood surface through a two-step hydrothermal process at 90 °C or 120 °C for 6 h. Chemical composition, crystalline structures, and morphologies of the WO_3-coated wood were characterized. The results indicated that the amount of WO_3 nanostructures on the surface of the wood substrate was 12.89 wt.%. Meanwhile, the WO_3 nanostructures were composed of fine nanoparticles and highly crystallized by SEM and XRD analysis. When the sample was irradiated under ultraviolet (UV) light (365 nm), there was an obvious color change after 10 min (ΔE). The water contact angle measurements demonstrated that the fluorosilane modified WO_3-coated wood surfaces possessed a superhydrophobic behavior with a contact angle of 152°. The sliding angle was less than 10°. Photochromic and superhydrophobic properties were achieved by a facile process, which could contribute to the development of functional wood with an aesthetic coloring.

INTRODUCTION

Wood is composed of a special supramolecular architecture that consists of cellulose, hemicellulose, and lignin in nature (Brostow *et al.* 2010). Due to its unique color, texture, and special aesthetic characteristics, it is popular and widely used in the furniture and decoration industries, amongst other plastic or metal materials (Janin *et al.* 2001; Mahraz 2011). In order to meet the increasing demands of wood, fast-growing wood species play an important role in the wood market. While fast-growing wood is generally characterized with light color and high brightness, historically there has been great preference to use wood with dark color in furniture manufacture and decoration. Therefore, different dyeing techniques had been used to visually improve the quality of wood.

The color and texture of wood are very important elements from the view of aesthetic appeal. Dyeing and coating are effective traditional methods that have been used to change the color of wood, but sometimes, by-products such as waste liquor and irritant gases are generated during the processes; in addition, organic dyes are somewhat unstable during sun exposure (Anex and Lund 1999; Hernandez and Cool 2008; Zhao *et al.* 2014). Therefore, there is still a motivation to develop green and stable methods to change the

color of wood. Many recent studies focused on changing the color of wood *via* the formation of inorganic photochromic nanomaterials on its surface by hydrothermal treatment, which has been regarded as a green process (Miyafuji *et al.* 2004; Wang *et al.* 2006; Salla *et al.* 2012; Sun *et al.* 2012a,b; Rao *et al.* 2016). Wang *et al.* (2006) reported that titanium dioxide coatings grown on the surface of wood could effectively improve the photostability of the substrate. Salla *et al.* (2012) reported that zinc oxide (ZnO) nanoparticles dispersed on the surface of wood can improve the color stability of the wood. Rao *et al.* (2016) also revealed that after layer-by-layer assembly of titanium dioxide (TiO$_2$) nanoparticles on the surface of wood, the brightness of wood was improved after UV irradiation. Therefore, the fabrication of inorganic photochromic materials on the surface of wood could be achieved by a simple process and could effectively change the color of the wood according to the consumers' demands.

Among those inorganic nanomaterials, tungsten dioxide (WO$_3$) films are interesting candidates due to their applicability as electrochromic devices and new signal amplifier devices, high sensitivity for gas sensor development, and field emission properties (Li *et al.* 2006; Huang *et al.* 2008; Khoo *et al.* 2010; Salla *et al.* 2012; Rao 2013). The WO$_3$ film can be synthesized using the sol-gel process, chemical vapor deposition, anodic oxidation, hydrothermal synthetization, or laser ablation (Djaoued *et al.* 2003; Lee *et al.* 2006; Wang *et al.* 2008; Meng *et al.* 2009). The various fabrication techniques for WO$_3$ nanostructures often used high temperatures. For example, Djaoued *et al.* (2003) reported the formation of WO$_3$ films with sol-gel methods and heated in the range 400 to 450 °C. Meng *et al.* (2009) reported the formation of WO$_3$ nanoparticles by annealing at 400-800 °C for 1 h, *etc*. Hui *et al.* (2015) reported on the hydrothermal synthetization of WO$_3$ nanosheets on the surface of wood. They also reported that WO$_3$ nanosheets were fabricated on the wood surface at 90 °C for 12 h, as shown in Table 1. Therefore, in our opinion, the fabrication of high quality WO$_3$ nanostructures with shorter time is still important from the view of both wood functionalization and energy conservation.

In this study, WO$_3$ nanoparticles were grown on wood surfaces through a low-temperature hydrothermal method at a short time. The chemical composition of the WO$_3$ layer was characterized by energy disperse spectroscopy (EDS), X-ray diffraction (XRD), and Fourier transform infrared spectroscopy (FTIR). The photochromic property of WO$_3$-coated wood was tested by evaluating the color change after being exposed to UV light. A superhydrophobic surface could be easily obtained by simply modification of inorganic nanomaterials coated wood. (Sun *et al.* 2011, Fu *et al.* 2012, Gan *et al.* 2015, *etc*.) Therefore, superhydrophobic wood was obtained after a simple fluoroalkyl silane modification to the WO$_3$-coated wood. A possible mechanism of the wood with photochromic and superhydrophobic properties is proposed. After the fabrication of WO$_3$ on the surface of the wood, the color of the wood was more similar to the color of valuable wood, having a yellowish and reddish saturated color. This work provides a further understanding of WO$_3$-coated wood and also offers promising market applications for fast-growing wood.

EXPERIMENTAL

Materials

Polar wood slices of size 20 mm × 20 mm × 10 mm were obtained from a plywood mill in Harbin, China. All of the specimens were ultrasonically rinsed with distilled water and ethanol for 30 min and subsequently dried in a vacuum oven at 60 °C for 48 h.

Tungstate chloride (WCl_6) (99.5%), anhydrous ethanol (99.7%), and acetone (99.5%) were purchased from Tianjin Kermel Chemical Reagent Co., Ltd. (Tianjin, China). The trimethoxy (1H,1H,2H,2H-heptadecafluorodecyl) silane used for surface hydrophobic modification was purchased from Shanghai Aladdin Chemical Co., Ltd. (Shanghai, China). All the chemicals were supplied without purification.

Methods

First, 0.06 M WCl_6 was dissolved in anhydrous ethanol for 30 min to obtain a clear liquid. The prepared wood samples were added to the above solution in an 80% filled Teflon stainless steel autoclave (Zhengzhou Keda Machinery and Instrument Equipment Co., Ltd., Zhengzhou, China). The autoclave was placed in an oven at 90 °C for 4 h and then cooled to room temperature.

Then, 0.025 M sodium dodecyl sulfonate (SDS) solution was added into the above solution with a volume ratio of 5%. The mixture was then heated to either 90 °C or 120 °C for 6 h. After cooling to room temperature, the samples were rinsed with ethanol and water several times and dried at 60 °C for 24 h. The obtained samples were labeled as S-temperature, *e.g.* S-90 or S-120, corresponding to the samples at 90 °C or 120 °C, respectively.

Characterization

The morphology and chemical compositions of the WO_3-coated wood surfaces were determined by a field emission scanning electron microscope (FE-SEM; JSM-7500, JEOL, Tokyo, Japan) at an operating voltage of 15 kV and an X-ray EDS (X-Max^N, Oxford Instruments, Oxford, UK). Transmission electron microscope (TEM) observation of the WO_3 nanostructure was performed using a JEM-2100 microscope (JEOL, Tokyo, Japan) at an acceleration voltage of 200 kV. Crystalline structures of the WO_3 nanostructures were identified by XRD (Rigaku D/max2200 diffractometer, Rigaku, Tokyo, Japan) using a CuKa radiation generator operated at a voltage of 40 kV and 30 mA. The FTIR spectroscopy (Nicolet, Thermo Fisher Scientific, Waltham, USA) was also utilized for characterizing the obtained samples using the attenuated total reflectance (ATR) mode.

The photochromic property of the WO_3-coated wood samples was tested using a color difference meter and digital photographs of the wood under the same light environment. The color change (ΔE) of the coated samples was characterized after exposure to a UV irradiation (365 nm) device (Dongguan Guangkai Instrument Co., Ltd., Guangzhou, China). The irradiated samples were also put in the dark for 24 h to test the recovery of the color. The Commission International de'Eclairage Lab (CIELAB) uniform color space for the color sheet system was used to calculate the color change using Eq. 1,

$$\Delta E = \sqrt{(\Delta L^*)^2 + (\Delta a^*)^2 + (\Delta b^*)^2} \qquad (1)$$

where L^*, a^*, and b^* are the three-dimensional rectangular coordinates, L^* refers to the lightness index, it varies from 100 (white) to 0 (black); while a^* and b^* are the chromaticity indices, $+a^*$ is the red direction, $-a^*$ is green; $+b^*$ is yellow, and $-b^*$ is blue, where ΔL^*, Δa^*, and Δb^* are the differences of initial and final values of a^*, b^*, and L^*.

The water contact angle was tested using an OCA20 contact angle tester (Dataphysics, Stuttgart, Germany). Before testing, the samples were modified by immersion into 50 mL ethanol solution with 5% trimethoxy (1H,1H,2H,2H-

bioresources.com

heptadecafluorodecyl) silane (v/v) at room temperature under continuous stirring for 24 h and then dried at 70 °C in a vacuum oven.

RESULTS AND DISCUSSION

Table 1 shows the conditions used for WO_3 synthesis in the present work, in comparison to earlier studies (Hui *et al.* 2015, 2016).

Table 1. Treatment Conditions Employed in Studies of Hydrothermally Synthesizes WO_3 on Wood Surfaces

Number	Tungsten precursor	Temperature / °C	Time / h	Products	Reference
1	WCl_6	90, 120	6	WO_3 nanoparticles	This work
2	Na_2WO_4 $2H_2O$	110	24	WO_3 nanosheets	Hui *et al.* 2016
3	Na_2WO_4 $2H_2O$	90	12	WO_3 nanosheets	Hui *et al.* 2015

The elemental composition and distribution on the surface of the wood was characterized using an X-ray EDS, as shown in Fig. 1. In Fig. 1a, there was a noticeable peak at approximately 1.8 keV, which corresponds to the tungsten (W) element. The mass percentage of W was 12.89%. It can be seen that the mapping images from Fig. 1b to 1d, W, carbon (C) and oxygen (O) had a uniform distribution on the surface of the wood. The EDS analysis revealed that the compounds containing W might have grown uniformly on the surface of wood.

Element	Wt.%	At.%
CK	43.49	56.46
OK	43.62	42.51
WK	12.89	1.03
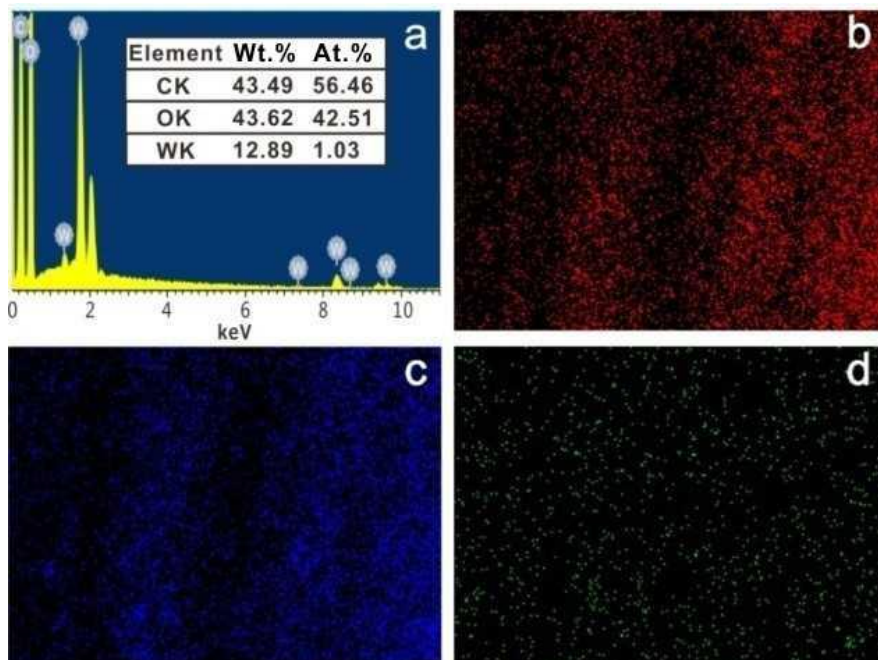
Fig. 1. EDS analysis of S-120 sample (a) and the mapping images of C elements (b), O elements (c), and W elements (d)

The samples that had been grown with tungsten compounds were further identified by XRD and FTIR analysis. As can be seen in Fig. 2, the XRD pattern highlights the crystalline structure of wood samples S-90 and S-120. As shown, the wood had two main peaks at around 18° and 23°, which corresponds to the typical cellulose peaks in wood (indicated by the green arrows). After growing tungsten compounds on the wood surface, some new peaks around 25°, 34°, 49°, and 56° appeared. The diffraction peaks were assigned to the (110), (201), (220), and (221) diffraction planes of hexagonal WO_3 structures (hexagonal WO_3, JCDScardno.75-2187, as indicated by the red arrows). For the high temperature sample (S-120), the peak intensity increased when compared to the lower temperature sample (S-90). This revealed the high crystallinity of WO_3 structures at high temperatures.
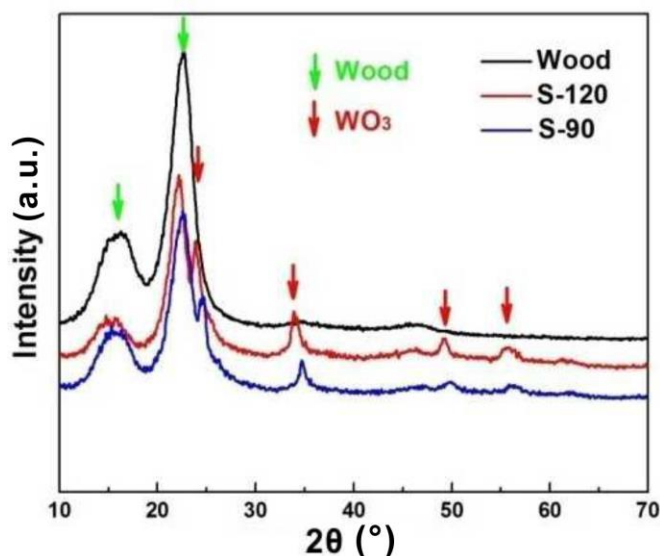
Fig. 2. XRD patterns of wood and WO_3-coated wood samples S-90 and S-120

The functional groups on the surface of wood were also characterized by FTIR, as shown in Fig. 3. The FTIR band at 3400 cm^{-1} was assigned to the O-H stretching mode of hydrogen-bonded hydroxyl groups or absorbed water, which is clearly reduced in the treated wood compared to that of the untreated wood (Fu *et al.* 2012). The FTIR band at 1735 cm^{-1} is attributed to C=O stretching in the non-conjugated aryl ketone of lignin carbonyl groups. The band at 1250 cm^{-1} is caused by C-O stretching in the phenolic hydroxyl group of lignin. These two bands were found in the spectrum of the original wood, but in the treated wood the two bands were weaker. This weakening was because wood was partially hydrolyzed during the hydrothermal process. The FTIR bands at 1460 cm^{-1} and 1506 cm^{-1} are assigned to the functional groups of lignin, and 1620 cm^{-1} is assigned to hemicellulose. The core components of wood were not changed in the hydrothermal process. However, when comparing the untreated and treated wood, there was a remarkable peak at 815 cm^{-1} in the curves of both the S-90 and S-120 samples that was not found in the untreated sample (Daniel *et al.* 1987; Guery *et al.* 1997). This peak is typically described as O–W–O stretching and bending modes of the bridging oxygen atoms in WO_3 (Hui *et al.* 2015). From the XRD and FTIR analyses, WO_3 was successfully fabricated on the surface of wood at both treatment temperatures (90 °C and 120 °C).
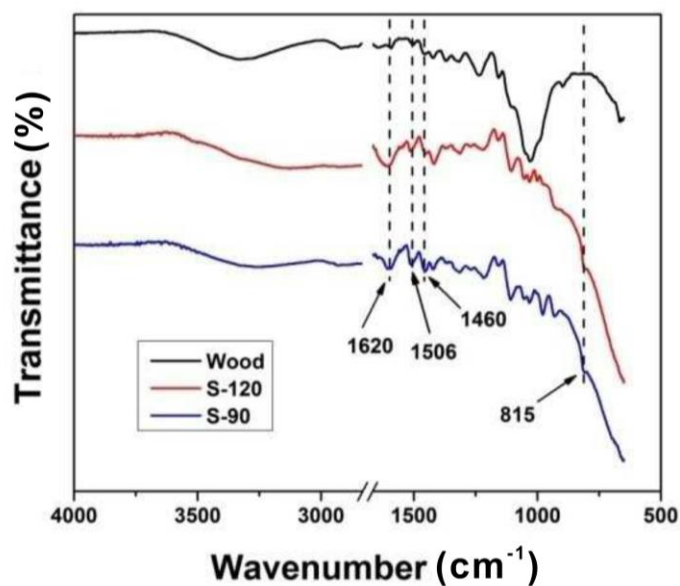
Fig. 3. FTIR spectra of untreated wood and WO_3-coated wood samples S-90 and S-120

The morphology of the WO_3 on the surface of the wood was observed by scanning electron microscopy (SEM). Figures 4a and 4b show that the surface of the untreated wood was smooth.
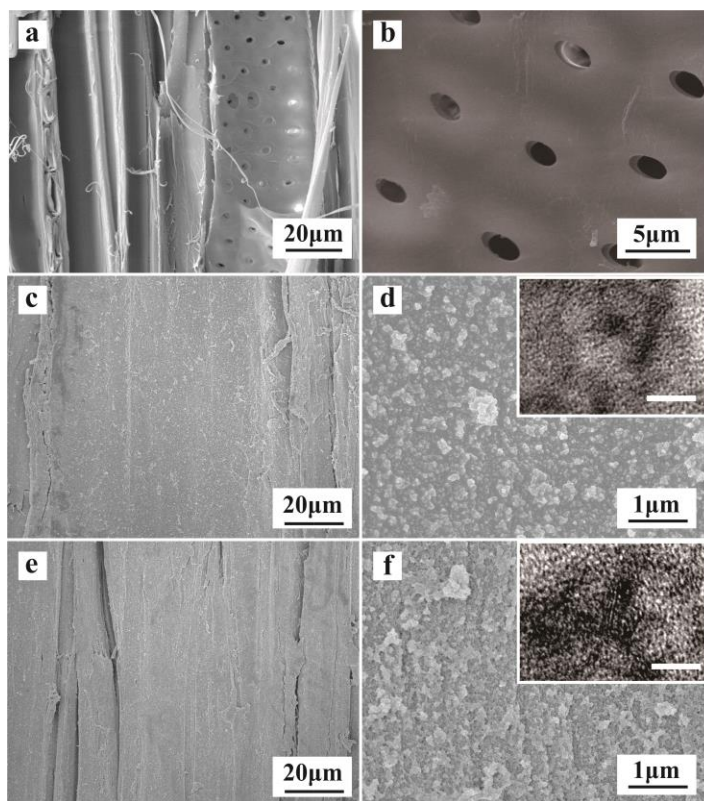
Fig. 4. SEM images of wood, S-90 and S-120 at low magnification (a, c, and e) and high magnification (b, d, and f) Insert: TEM images of the WO_3 nanoparticles, the scale bar is 5 nm

bioresources.com

The wood cell and pit structures can be seen clearly. However, after growing WO_3 on the surface of the wood at 90 °C, the surface was covered with a layer, and the microstructure of the wood cannot be seen (Fig. 4c). At high magnification (Fig. 4d), it can be seen that the WO_3 layer was composed of many nanoparticles and was distributed quite evenly. The WO_3 layer became thicker after increasing the temperature to 120 °C, as can be seen in Figs. 4e and 4f. The density of the WO_3 nanoparticles increased with increased temperature. This can possibly be attributed to the fact that WO_3 grows better at relatively high temperatures. The structure of the WO_3 on wood surface was also characterized by TEM. We can see in the insert TEM images that at 120 ºC, the WO_3 nanoparticles were with higher crystallinity structures. This result agreed with that obtained from the XRD analysis. The results showed that crystalline WO_3 nanoparticles were hydrothermally grown on wood surface at a low temperature of 90 °C; meanwhile, the reaction time was comparable as compared with the previous literature (Gavrilyuk 1999; Hui *et al.* 2015). The WO_3 nanoparticles were successfully grown on the wood surface through facile and relatively mild hydrothermal conditions.

The results of the color change of untreated and treated wood (samples S-90 and S-120) before and after UV irradiation are shown in Figs. 5 and 6. The brightness (L) of S-90 and S-120 decreased 32.8% and 47.2% compared to the untreated sample, respectively. This revealed that after the coating with WO_3, the wood became darker. This is obvious in the photographs in Fig. 5.

Fig. 5. Photographs of untreated wood, S-90, and S-120 before and after 6 h UV irradiation

However, as shown in Fig. 6, the *a** value of the S-90 sample group decreased remarkably (70.8%) after the coating process, while the S-120 sample group remained stable. This result demonstrated that at a low temperature, the coating had a tendency to take on a greener color, while at a high temperature the color remained unchanged when compared to the untreated wood. The *b** value changed very little for both the S-90 and S-120 samples. It can be concluded from the above results that the WO_3 coating had a

remarkable dyeing effect on wood at a low temperature. At a high temperature, the color values remained stable but the brightness changed.

The photochromic property of the WO_3-coated wood was tested after 6 h of UV irradiation. The brightness of the untreated wood and the S-90- and S-120-coated samples changed minimally in Fig. 6a. However, for the S-90 sample, the $a*$ value improved after UV radiation, increasing 600% in Fig. 6b. The $b*$ value also increased for the S-90 sample. For the S-120 sample, the $a*$ value increased while the $b*$ value decreased after UV radiation. The results revealed that the color of the S-90-coated wood sample became darker, redder, and more yellow after 6 h of UV radiation, which was similar to that of traditional high-grade wood. The S-120-coated wood sample became redder and bluer. After the growth of WO_3 nanoparticles on the surface of the wood at 90 °C, the value of ΔE was lowest compared to the untreated wood and S-120. This color change was attributed to the photochromic property of the WO_3 layer on the surface of the wood. The color change was more obvious in the higher-temperature sample, S-120, compared to that of the lower-temperature S-90 sample in Fig. 6d. This difference in color change based on temperature was attributed to the thicker growth of the WO_3 layer at a higher temperature. Therefore, the WO_3 layer on wood surface was sensitive to UV light, though this result was not permanent.
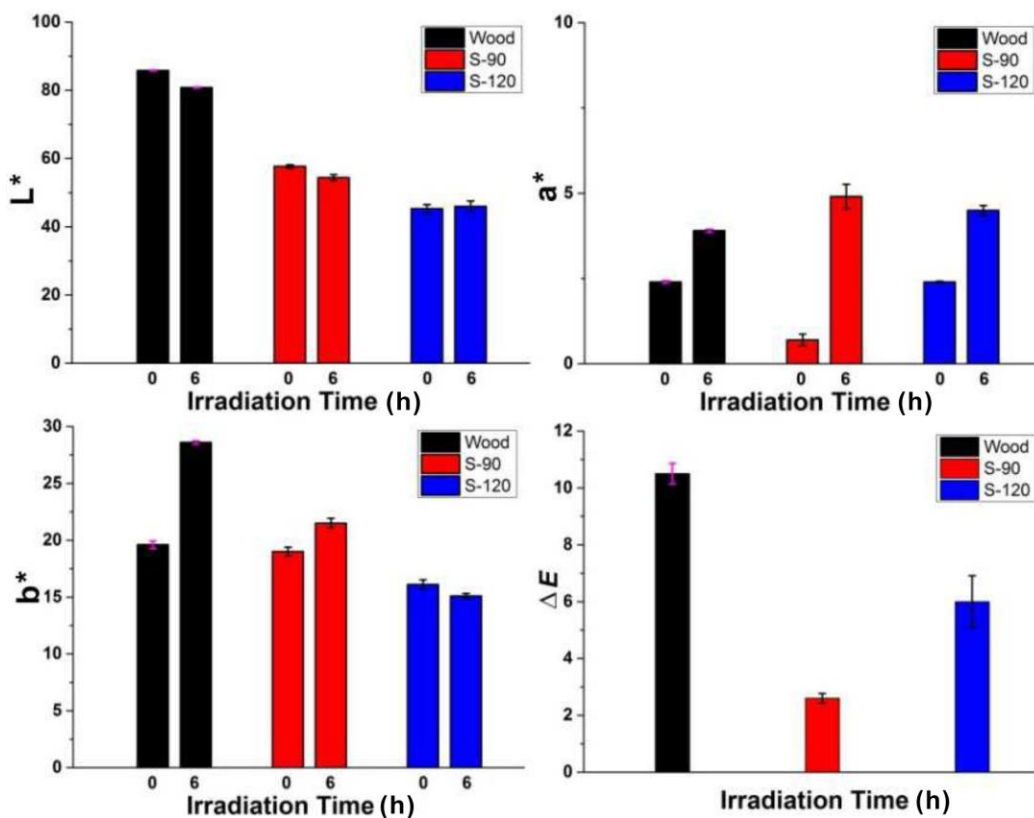
Fig. 6. Color parameters (L, a*, b*, and ΔE) of untreated wood and treated samples S-90 and S-120 before and after 6 h of UV irradiation

After 24 h in a dark environment, the color was recovered. The results were similar to the literature (Hui *et al.* 2016). This will be considered with further experiments in the future. The results of photochromic properties of WO_3-coated wood was due to the

bioresources.com

following scheme: after UV radiation, the WO_3 layer on wood surface was excited after an electron injection process and a further reaction, and then a pair of electrons and holes formed, as shown in Fig. 7a. The WO_3 layer turned blue due to the inter-valence charge transfer from the valence band of $W5^+$ to the conduction band of $W6^+$, as reported in previous literature (Su *et al.* 2010; Chai *et al.* 2014).
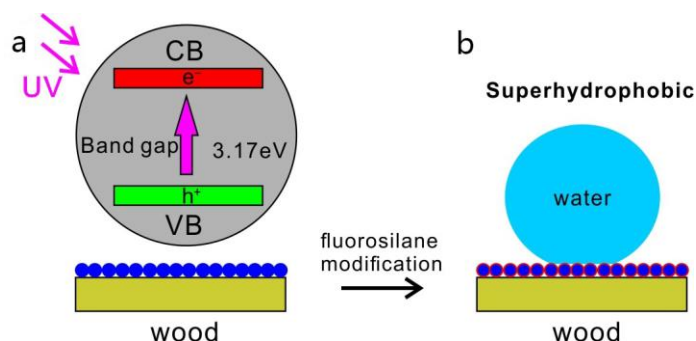
Fig. 7. Schematic diagram of WO_3 coated wood surface with photochromic and superhydrophobic property

The modification of hydrophobicity in the S-90 and S-120 samples compared to the untreated wood is shown in Fig. 8. The untreated wood had an initial contact angle of 80°, and it dropped to 30° after 60 s (Fig. 8a). However, the S-90 sample had an initial contact angle of 146° that remained stable at 145° after 60 s (Fig. 8b). The initial contact angle of the S-120 sample was 152° and remained stable after 60 s. Superhydrophobicity of the WO_3-coated wood was achieved, as shown in Figs. 8c and 8d. The S-120 sample had a sliding contact angle of less than 10°. To further understand the wetting behavior of the wood samples, the Wenzel and the Cassie and Baxter state models were applied (Boussu *et al.* 2005; Erbil and Cansoy 2009; Shen *et al.* 2015). The Wenzel model assumes that a liquid completely fills the grooves where it contacts the substrate.
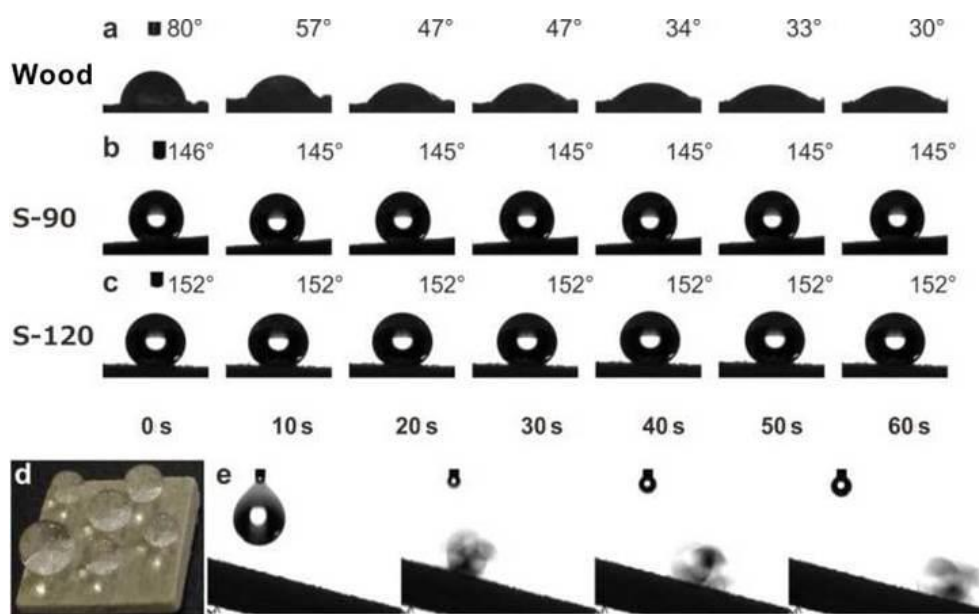
Fig. 8. Water contact angle (WCA) of untreated wood (a), S-90 (b), and S-120 (c) within 60 s, digital images of water droplets on the S-120 sample surface (d), and sliding angle images of modified S-120 (e)

bioresources.com

For the Cassie and Baxter state model, an air pocket is trapped in the groove of the textured surface and a liquid "sits" on the surface (Liu *et al.* 2013; Wang *et al.* 2014; Guo *et al.* 2017). In this study, wood as a hydrophilic material (Fig. 7b), allowed water droplets to fill the grooves on its surface, which resulted in a low contact angle and after some time the water was absorbed into the wood. However, after the growth of WO_3 nanoparticles on the surface of the wood, the wood surface became hydrophobic and rough; the Cassie and Baxter model is formed and the water droplet stays stable on the surface. For the S-120 sample, the WO_3 layer was thicker and rougher compared to S-90, and a Cassie-Baxter state model was formed, which resulted in a superhydrophobic surface that allowed the water droplets to slide on the surface (Fig. 8e).

In summary, the photochromic and superhydrophobic properties were obtained by a simple hydrothermal method. For the photochromic property, it has potential applications in information storage and light sensor. After a simple modification with low surface energy materials, it also has the self-cleaning property. We also hope that the WO_3-coated wood can combine with paints for outdoor application or combine with wax, which is also widely used on furniture for indoor application. In addition, the thermal and mechanical properties are also important for application. These aspects will be considered in further experimental studies.

CONCLUSIONS

1. Wood with photochromic and superhydrophobic properties was achieved by hydrothermally growing WO_3 nanoparticles on the surface of the wood at a low temperature. The SEM images proved that temperature played a key role in the thickness and roughness of the WO_3 layer.

2. The WO_3-coated wood was sensitive to UV light and was more sensitive at a high temperature of 120 °C.

3. Self-cleaning character was obtained after a simple fluorosilane modification of the WO_3-coated wood.

4. This study provides a simple and mild method for enhancing the visual quality of fast-growing wood. Changing the reaction conditions and photo stimulation controlled the color.

ACKNOWLEDGMENTS

REFERENCES CITED

Anex, R. P., and Lund, J. R. (1999). "Bayesian estimation of volatile organic emissions from wood furniture coating," *Journal of Environmental Engineering* 125(1), 92-96. DOI: 10.1061/(ASCE)0733-9372(1999)125:1(92)

Boussu, K., Van, d. B. B., Volodin, A., Snauwaert, J., Van, H. C., and Vandecasteele, C. (2005). "Roughness and hydrophobicity studies of nanofiltration membranes using different modes of AFM," *Journal of Colloid Interface Science* 286(2), 632-638. DOI: 10.1016/j.jcis.2005.01.095

Brostow, W., Datashvili, T., and Miller, H. (2010). "Wood and wood derived materials," *Journal of Materials Education* 32(3), 125-138.

Chai, B., Li, J., Xu, Q., and Dai, K. (2014). "Facile synthesis of reduced graphene oxide/WO_3 nanoplates composites with enhanced photocatalytic activity," *Materials Letters* 120(1), 177-181. DOI: 10.1016/j.matlet.2014.01.094

Daniel, M. F., Desbat, B., Lassegues, J. C., Gerand, B., and Figlarz, M. (1987). "Infrared and Raman study of WO_3 tungsten trioxides and WO_3, xH_2O tungsten trioxide tydrates," *Journal of Solid State Chemistry* 67(2), 235-247. DOI: 10.1016/0022-4596(87)90359-8

Djaoued, Y., Ashrit, P. V., Badilescu, S., and Brüning, R. (2003). "Synthesis and characterization of macroporous tungsten oxide films for electrochromic application," *Journal of Sol-Gel Science and Technology* 28(2), 235-244. DOI: 10.1023/A:1026089318607

Erbil, H. Y., and Cansoy, C. E. (2009). "Range of applicability of the Wenzel and Cassie-Baxter equations for superhydrophobic surfaces," *Langmuir* 25(24), 14135-14145. DOI: 10.1021/la902098a

Fu, Y., Yu, H., Sun, Q., Li, G., and Liu, Y. (2012). "Testing of the superhydrophobicity of a zinc oxide nanorod array coating on wood surface prepared by hydrothermal treatment," *Holzforschung* 66(6), 739-744. DOI: 10.1515/hf-2011-0261

Gan, W., Gao, L., Sun, Q., Jin, C., Lu, Y., and Li, J. (2015). "Multifunctional wood materials with magnetic, superhydrophobic and anti-ultraviolet properties," *Applied Surface Science*, 332, 565-572. DOI: 10.1016/j.apsusc.2015.01.206

Gavrilyuk, A. I. (1999). "Photochromism in WO_3 thin films," *Electrochimica Acta* 44(18), 3027-3037. DOI: 10.1016/S0013-4686(99)00017-1

Guery, C., Choquet, C., Dujeancourt, F., Tarascon, J. M., and Lassègues, J. C. (1997). "Infrared and X-ray studies of hydrogen intercalation in different tungsten trioxides and tungsten trioxide hydrates," *Journal of Solid State Electrochemistry* 1(3), 199-207. DOI: 10.1007/s100080050049

Guo, B., Liu, Y., Zhang, Q., Wang, F., Wang, Q., Liu, Y., Li, J., and Yu, H. (2017). "Efficient flame-retardant and smoke-suppression properties of Mg–Al layered double hydroxide nanostructures on wood substrate," *ACS Applied Materials & Interfaces* 9(27), 23039-23047. DOI: 10.1021/acsami.7b06803

Hernandez, R. E., and Cool, J. (2008). "Evaluation of three surfacing methods on paper birch wood in relation to water-and solvent-borne coating performance," *Wood and Fiber Science* 40(3), 459-469.

Huang, K., Pan, Q., Yang, F., Ni, S., Wei, X., and He, D. (2008). "Controllable synthesis of hexagonal WO_3 nanostructures and their application in lithium batteries," *Journal of Physics D: Applied Physics* 41(15), 155417. DOI: 10.1088/0022-3727/41/15/155417

Hui, B., Wu, D., Huang, Q., Cai, L., Li, G., Li, J., and Zhao, G. (2015). "Photoresponsive and wetting performances of sheet-like nanostructures of tungsten trioxide thin films grown on wood surfaces," *RSC Advances* 5(90), 73566-73574. DOI: 10.1039/C5RA10479C

Hui, B., Li, G., Li, J., and Via, B. K. (2016). "Hydrothermal deposition and photoresponsive properties of WO_3 thin films on wood surfaces using ethanol as an assistant agent," *Journal of the Taiwan Institute of Chemical Engineers* 64, 336-342. DOI: 10.1016/j.jtice.2016.04.031

Janin, G., Gonçalez, J. C., Ananías, R. A., Charrier, B., Silva, G. F., and Dilem, A. (2001). "Aesthetics appreciation of wood colour and patterns by colorimetry: Part 1. Colorimetry theory for the CIELab system," *Maderas. Ciencia y Tecnología* 3(1-2), 3-13. http://repositorio.unb.br/handle/10482/10498

Khoo, E., Lee, P. S., and Ma, J. (2010). "Electrophoretic deposition (EPD) of WO_3 nanorods for electrochromic application," *Journal of the European Ceramic Society* 30(5), 1139-1144. DOI: 10.1016/j.jeurceramsoc.2009.05.014

Lee, S. H., Deshpande, R., Parilla, P. A., Jones, K. M., To, B., Mahan, A. H., and Dillon, A. C. (2006). "Crystalline WO_3 nanoparticles for highly improved electrochromic applications," *Advanced Materials* 18(6), 763-766. DOI: 10.1002/adma.200501953

Li, X., Zhang, G., Cheng, F., Guo, B., and Chen, J. (2006). "Synthesis, characterization, and gas-sensor application of WO_3 nanocuboids," *Journal of the Electrochemical Society* 153(7), H133-H137. 0013-4651/2006/153(7)/H133/5/

Liu, Y., Fu, Y., Yu, H., and Liu, Y. (2013). "Process of *in situ* forming well-aligned zinc oxide nanorod arrays on wood substrate using a two-step bottom-up method," *Journal of Colloid & Interface Science* 407(1), 116-121. DOI: 10.1016/j.jcis.2013.06.043

Mahraz, U. E. (2011). "A screening study of natural colour of wood from different geographical regions," *Research Journal of Forestry* 5(4), 162-168. DOI: 10.3923/rjf.2011.162.168

Meng, D., Yamazaki, T., Shen, Y., Liu, Z., and Kikuta, T. (2009). "Preparation of WO_3 nanoparticles and application to NO_2 sensor," *Applied Surface Science* 256(4), 1050-1053. DOI: 10.1016/j.apsusc.2009.05.075

Miyafuji, H., Kokaji, H., and Saka, S. (2004). "Photostable wood–inorganic composites prepared by the sol-gel process with UV absorbent," *Journal of Wood Science* 50(2), 130-135. DOI: 10.1007/s10086-003-0550-x

Rao, M. C. (2013). "Structure and properties of WO_3 thin films for electrochromic device application," *Journal of Non-Oxide Glasses* 5(1), 1-8.

Rao, X., Liu, Y., Fu, Y., Liu, Y., and Yu, H. (2016). "Formation and properties of polyelectrolytes/TiO_2 composite coating on wood surfaces through layer-by-layer assembly method," *Holzforschung* 70(4), 361-367. DOI: 10.1515/hf-2015-0047

Salla, J., Pandey, K. K., and Srinivas, K. (2012). "Improvement of UV resistance of wood surfaces by using ZnO nanoparticles," *Polymer Degradation and Stability* 97(4), 592-596. DOI: 10.1016/j.polymdegradstab.2012.01.013

Shen, W., Zhang, C., Li, Q., Zhang, W., Cao, L., and Ye, J. (2015). "Preparation of titanium dioxide nanoparticle modified photocatalytic self-cleaning concrete," *Journal of Cleaner Production* 87(15), 762-765. DOI: 10.1016/j.jclepro.2014.10.014

Su, J., Feng, X., Sloppy, J. D., Guo, L., and Grimes, C. A. (2010). "Vertically aligned WO_3 nanowire arrays grown directly on transparent conducting oxide coated glass: Synthesis and photoelectron chemical properties," *Nano Letters* 11(1), 203-208. DOI: 10.1021/nl1034573

Sun, Q., Lu, Y., Zhang, H., Yang, D., Wang, Y., Xu, J., Tu, J., Liu, Y., and Li, J. (2012a). "Improved UV resistance in wood through the hydrothermal growth of highly ordered ZnO nanorod arrays," *Journal of Material Science* 47(10), 4457-4462. DOI: 10.1007/s10853-012-6304-7

Sun, Q., Lu, Y., Zhang, H., Zhao, H., and Yu, H. (2012b). "Hydrothermal fabrication of rutile TiO_2 submicrospheres on wood surface: An efficient method to prepare UV-protective wood," *Material Chemistry & Physics* 133(1), 253-258. DOI: 10.1016/j.matchemphys.2012.01.018

Sun, Q., Lu, Y., and Liu, Y. (2011). "Growth of hydrophobic TiO_2 on wood surface using a hydrothermal method," *Journal of Materials Science* 46(24), 7706-7712. DOI: 10.1007/s10853-011-5750-y

Wang, G., Ji, Y., Huang, X., Yang, X., Gouma, P., and Dudley, M. (2006). "Fabrication and characterization of polycrystalline WO_3 nanofibers and their application for ammonia sensing," *Journal of Physical Chemistry B* 110(47), 23777-23782. DOI: 10.1021/jp0635819

Wang, J., Khoo, E., Lee, P. S., and Ma, J. (2008). "Synthesis, assembly, and electrochromic properties of uniform crystalline WO_3 nanorods," *Journal of Physics Chemistry C* 112(37), 14306-14312. DOI: 10.1021/jp804035r

Wang, N., Fu, Y., Liu, Y., Yu, H., and Liu, Y. (2014). "Synthesis of aluminum hydroxide thin coating and its influence on the thermomechanical and fire-resistant properties of wood," *Holzforschung* 68(7), 781-789. DOI: 10.1515/hf-2013-0196

Zhao, Y., Tan, X., Wan, X., Yuan, Y., Yu, Z., and Tang, J. (2014). "Dyeing of acetylated wood with disperse dyes," *Wood and Fiber Science* 46(3), 401-411.